Nuclear Reactions Induced by a Pyroelectric Accelerator

Jeffrey Geuther,* Yaron Danon, and Frank Saglime

Department of Mechanical, Aerospace, and Nuclear Engineering, Rensselaer Polytechnic Institute, Troy, New York 12180, USA

(Received 21 October 2005; published 9 February 2006)

This work demonstrates the use of pyroelectric crystals to induce nuclear reactions. A system based on a pair of pyroelectric crystals is used to ionize gas and accelerate the ions to energies of up to 200 keV. The system operates above room temperature by simply heating or cooling the pyroelectric crystals. A D-D fusion reaction was achieved with this technique, and 2.5 MeV neutrons were detected. The measured neutron yield is in good agreement with the calculated yield. This work also verifies the results published by Naranjo, Gimzewski, and Putterman [Nature (London) **434**, 1115 (2005)].

DOI: 10.1103/PhysRevLett.96.054803 PACS numbers: 29.25.Dz, 77.70.+a

Pyroelectric crystals are spontaneously polarized under equilibrium conditions, and experience a change in polarization when heated or cooled. While at atmospheric pressure this change is quickly masked by the accumulation of charges from the air, in vacuum the change in polarization is unmasked, and the resulting surface charge results in an electric field. The material-specific constant dictating the change in surface charge density per degree change in temperature is the pyroelectric coefficient φ, and is typically expressed in units of $\mathrm{C}/(\mathrm{m}^2\,\mathrm{K})$. Lithium tantalate ($LiTaO_3$) has a particularly high pyroelectric coefficient, $\varphi = 190\ \mu\mathrm{C}/(\mathrm{m}^2\,\mathrm{K})$ [1].

By modeling a crystal and the gap between the crystal and its target as a system of parallel plate capacitors, we see that the potential created between the crystal and the target should equal the charge divided by the capacitance, $V = Q/\mathrm{C}$. By substituting the charge created via the pyroelectric effect for Q, and assuming that the loss of charge due to screening, leakage current, and electron emission is small, we obtain $V = (\varphi \Delta T)/(\epsilon_{\mathrm{cr}}/d_{\mathrm{cr}} + \epsilon_o/d_{\mathrm{gap}})$ [2,3]. In practice, the distance between the crystal and target is of little significance, since $\epsilon_{\mathrm{cr}} \gg \epsilon_o$. (For $LiTaO_3$, $\epsilon_{\mathrm{cr}} = 46\epsilon_o$). Therefore, the thickness of the crystal, d_{cr}, dominates the denominator, and we find that maximum potential in a pyroelectric source is an almost linear function of crystal thickness, although for $d_{\mathrm{cr}} > 1$ cm, the potential is found to no longer increase significantly with thickness [3]. In previous work, we have shown that the maximum potential can be doubled by using a second pyroelectric crystal of opposite polarity to the emitting crystal [3,4]. The maximum electron energy in a two-crystal system has been found to be 215 keV [4].

Only one of the two possible D-D fusion reactions produces neutrons. The cross section for D-D fusion is effectively zero below 20 keV, and reaches 16.3 mb at 100 keV [5]. Therefore, the electric field created in a paired-crystal pyroelectric source is strong enough to induce D-D fusion. While pyroelectric crystals have long been known to be useful for x-ray generation [6,7], and have been shown to produce positive ions [8,9], the use of pyroelectric crystals for neutron generation is a new technique [10–13]. Previous work [10] was done using a single 30 mm diameter $\times 10$ mm thick $LiTaO_3$ crystal, which was cooled below room temperature (240–280 K) with liquid nitrogen. The maximum acceleration potential for this system was below 110 keV. In this work we introduced two important new features in pyroelectric neutron generation technology. First, we extended our research of paired-crystal pyroelectric electron accelerators [4] to show that such a system can also be used to accelerate deuterium ions. Also, we used low-power thermoelectric heaters [14] to drive the accelerator by heating two crystals to 130 °C and then allowing them to cool to room temperature. We were therefore able to produce fusion neutrons without using cryogenic cooling used in the previous work [10].

Our experiments were performed using two 10 mm thick, 20 mm diameter $LiTaO_3$ crystals, as shown in Fig. 1. Both crystals were attached to thermoelectric heaters using electrically conductive epoxy (GC Electronics #19-2092-0000). A copper strip was pressed between each crystal and its thermoelectric heater to provide electrical ground. Temperature indication was provided by a chromel-alumel thermocouple epoxied to one of the thermoelectric heaters. The thermoelectric heaters were attached to a copper heat sink using nylon screws. The crystal with the exposed $z-$ surface, which exhibits a positive charge during heating and a negative charge during cooling, was coated with deuterated polystyrene $-[(C_8D_8)_n-]$. The thickness of the deuterated polystyrene layer was about 50 μm. The crystal with the exposed $z+$ surface, which exhibits a negative charge during heating and a positive charge during cooling, was partially covered by a 13 mm diameter, 1 mm thick copper disk, which was attached to the crystal using the electrically conductive epoxy. A 3 mm long tungsten catwhisker probe tip with a 0.07 μm tip radius [15] was soldered to the center of the disk, normal to the surface [10]. The catwhisker tip was used to enhance the electric field in the region around the tip to improve the gas ionization rate. The crystals were oriented parallel to each other at a separation distance of 15 mm. Similar experiments performed with a tungsten tip

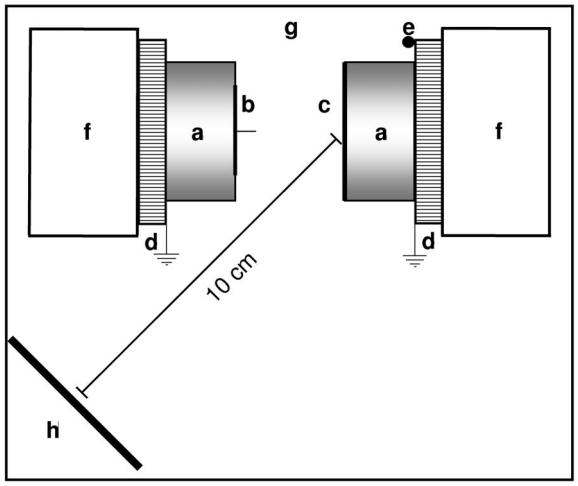

FIG. 1. Setup for paired-crystal neutron generation experiments. (a) 20 mm dia. $\times$ 10 mm thick $LiTaO_3$ crystal. (b) 3 mm long catwhisker tip with 0.07 μm apex mounted to a 13 mm dia. $\times$ 1 mm thick Cu disk. (c) Deuterated polystyrene target. (d) Thermoelectric heater/cooler. (e) Thermocouple. (f) Cu heat sink. (g) Vacuum chamber filled with 1.2 mTorr D_2 gas. (h) $3'' \times 3''$ EJ-301 detector at 45° angle to crystals.

with a 600 nm apex radius, as well as experiments performed with no tip, did not produce a measurable neutron yield.

The crystals and heat sink were placed in a vacuum chamber, which was pumped down to a base pressure of 1 μTorr. The chamber was then filled with deuterium gas. The final pressure was 1.2 mTorr for the most successful experiments. Increasing the pressure to 10 mTorr resulted in a reduction of neutron yield by approximately a factor of 2. Experiments conducted at pressures below 0.7 mTorr did not result in an observable neutron yield. Each crystal was heated with 10 W of power to 130 °C over 350 seconds, and then cooled to room temperature by switching off the power to the thermoelectric heater.

Neutron detection was performed using a 76 mm diameter $\times$76 mm thick proton-recoil detector (Eljen model 510-30X30X-3/301). This detector was located outside the vacuum chamber, at a distance of 100 mm from the deuterated target. The detector was shielded by a 50 mm thick lead shield on all sides except for the back of the photomultiplier tube, which was exposed to allow cable connections, and the front of the liquid scintillator vessel, which was wrapped with a 1 mm lead sheet. Since electrons bombarded the ion-emitting crystal during the cooling phase, neutron production was accompanied by strong bremsstrahlung x-ray production. The x rays and background photons were discriminated against using pulse-shape discrimination. The pulse-shape discrimination reduced the observed rate from a ^{22}Na calibration source by a factor of 650.

An Amptek XR-100T-CdTe semiconductor diode detector was used to collect x-ray spectra. It had an active area of 3 mm $\times$ 3 mm and was located 180 mm from the center of the crystals. It was shielded by a 5 mm thick glass window. Using the x-ray spectra recorded with this detector, we were able to estimate the potential difference between the crystals, since the end point energy of a bremsstrahlung continuum is equal to the maximum electron energy, and the energy of an electron is equal to the charge of the electron times the potential through which it is accelerated [4]. In addition to pulse-height spectra, the x-ray count rate as a function of time was recorded. This gave indication of when the charge on the crystals was neutralized by electrostatic breakdown.

Figure 2 shows the summed net neutron emission spectra from three cooling phases. The background spectrum is shown for reference. The end point energy of the neutron continuum in Fig. 2 corresponds to the maximum light output from a liquid scintillator after the proton recoil from an incident 2.5 MeV (i.e., D-D fusion) neutron [16].

The neutron detector energy scale was calibrated with reference to the Compton edges of a ^{22}Na gamma source, and thus is given in units of MeV_e [16]. Data available from a time-of-flight experiment were used to generate a reference 2.5 MeV neutron spectrum. For the time-of-flight experiment, a linear accelerator was used to generate a 30 ns pulse of 50 MeV electrons incident on a tantalum bremsstrahlung target. The resulting bremsstrahlung radiation then produced neutrons via a (γ, n) reaction with the tantalum. The detector was placed 31.237 m away from the target and a narrow time window (corresponding to 0.1 MeV) was used to discriminate neutrons of the proper energy. The detection system combined a state of the art digitizer with modern software to process the digital signals from a $5'' \times 3''$ EJ-301 liquid scintillator with a response function similar to the $3'' \times 3''$ EJ-301 detector

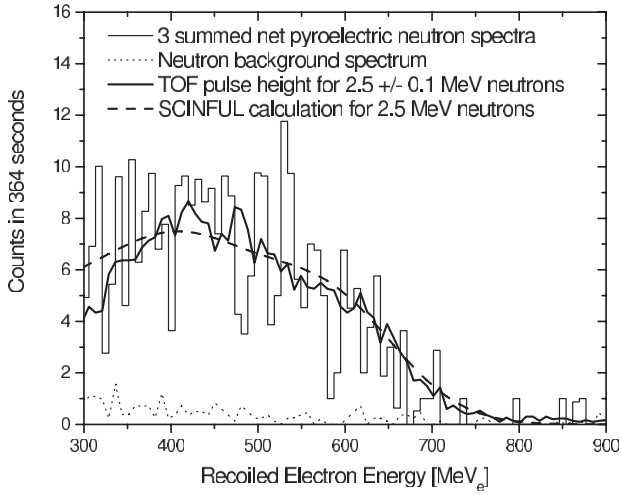

FIG. 2. Net neutron pulse-height spectrum compared with a background radiation spectrum, a SCINFUL [17] simulation of 2.5 MeV neutrons in a NE-213 scintillator, and a reference spectrum generated by time-of-flight method.

used in this experiment. The reference spectrum generated in the time-of-flight experiment is included in Fig. 2. Figure 2 also includes a SCINFUL [17] calculation of the detector response pulse-height spectrum from 2.5 MeV neutrons, and shows good agreement with our experimental results.

Figure 3 shows the x-ray emission that accompanied the neutron production shown in Fig. 2. The end point x-ray energy is 200 keV, which indicates a 200 kV potential difference between the emitting crystal and target crystal.

Figure 4 shows the change in x-ray count rate with respect to time. The count rate is correlated to the electric field strength. Note that the count rate increases rapidly, and then reaches a quasiequilibrium value. Figure 4 also shows the occurrence of electrostatic discharge, evident from the drop in count rate from 4000 counts per second to zero.

In successful neutron production experiments, we typically observed 154 ± 7 gross counts per heating cycle in a region of interest from 0.2 MeV_e to 1.0 MeV_e. The average emission time was 120 seconds. The background in our region of interest was 0.14 ± 0.01 counts per second. Therefore, our typical successful experiment yielded approximately 138 ± 7 net neutron counts. Our neutron detector, as stated before, was located 100 mm away from the center of the emitting crystal, and had a diameter of 76 mm. The total number of neutron emission events, S, can be estimated as [18]:

$$S = 4\pi N/\eta\Omega, \tag{1}$$

where N is the observed number of events, η is the intrinsic detector efficiency, and Ω is the solid angle. By approximating our target as an isotropically emitting point source, we find the solid angle to be:

$$\Omega = 2\pi(1 - d/\sqrt{d^2 + a^2}), \tag{2}$$

where d is the distance from the point source to the detector and a is the detector radius. We substitute in our values, $d = 100$ mm, and $a = 38$ mm, and find $\Omega = 0.41$. Using SCINFUL [17], we found our intrinsic neutron detector efficiency for 2.5 MeV neutrons (with pulses rejected below 0.2 MeV_e) to be $\eta = 0.4$. Using this value for intrinsic efficiency, and our average total number of observed neutrons, we find our total number of neutrons produced by D-D fusion to be $S = 10\,574 \pm 536$.

It is not clear whether the ionization of the deuterium fill gas in the vicinity of the tip results in the formation of a single D_2^+ ion or if the electric field in this region is strong enough to form two D^+ ions. In the case of D_2^+, each ion would only have half of the total kinetic energy of the molecule, so for an accelerating potential of 200 kV we would only accelerate the ions to 100 keV. If the molecule separates during ionization, each D^+ ion would accelerate to 200 keV.

When the deuterons created by the ionization of the deuterium gas travel into the deuterated polystyrene target, they lose energy through Coulombic interaction with the target ions. Therefore, the cross section for fusion gradually decreases as the deuteron penetrates the target, with the cross section of a 100 keV incident deuteron falling below 0.27 mb after penetrating 1 μm into the target. Therefore, our 50 μm target is sufficient to stop the deuterons completely.

Assuming that the incident deuterons are monoenergetic, the neutron production rate inside the target is:

$$R(x)dx = \phi(x)N\sigma[E(x)]dx, \tag{3}$$

where $\phi(x)$ is the ion flux through the entire target surface, $E(x)$ is the energy of the incident ion at depth x, $N(x)$ is the number density of deuterium ions in the target, and $\sigma[E(x)]$ is the microscopic D-D fusion cross section. The cross section is a function of energy, and the energy of the incident deuterons is itself a function of penetration depth. By assuming that the ion flux is independent of the pene-

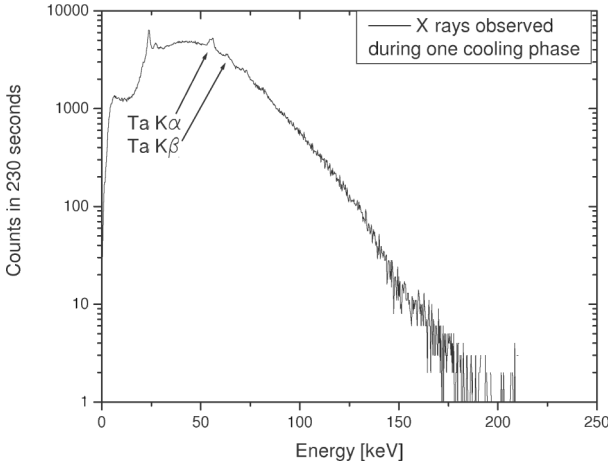

FIG. 3. X-ray spectrum recorded during a neutron emission phase.

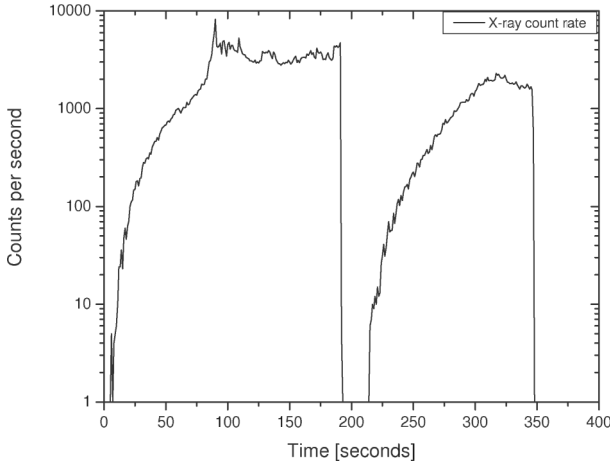

FIG. 4. X-ray counts per second observed during a neutron emission phase.

tration depth, we can integrate over the penetration depth to find the total production rate:

$$R = \phi N \int \sigma[E(x)]dx, \tag{4}$$

where $E(x)$, the energy at depth x and is given by:

$$E(x) = E_0 - \int_0^x \frac{dE}{dx}(x)dx. \tag{5}$$

$dE/dx(x)$ for deuterated polystyrene was found using the Monte Carlo code SRIM [19]. It has been observed that the maximum positive ion energy in a pyroelectric source is somewhat less than the maximum electron energy [9]. It can be seen from our x-ray spectra that our source is capable of producing 200 keV electrons, so it is reasonable to assume that we can produce at least 100 keV D^+ ions. If we assume that the ions are emitted at 100 keV for 100 seconds, our estimate of the total neutron emission per nA ion current, $\Re$, becomes:

$$\Re = 6.25 \times 10^{11} \text{ ions} \times N \int \sigma[E(x)]dx. \tag{6}$$

By integrating numerically over the penetration depth we find the integrated cross section for a 100 keV ion to be $64.1b$ Å. Entering our value for N, $N = 4.73 \times 10^{-10}$ per barn Angstrom, we get $\Re = 18\,950$ neutrons per heating cycle per nA. This number is slightly greater than experimentally observed neutron source strength of about 10 500 neutrons per cooling phase, and implies that the ion current in our experiment was 0.55 nA.

In conclusion, we were successful in producing fusion neutrons by ionizing a dilute deuterium fill gas with the strong electric field between two polarized pyroelectric crystals, and accelerating the deuterons into a deuterated polystyrene target at energies above the threshold for fusion. This effect was observed without the need for cryogenic cooling of the crystals. Our neutron yield agrees to first order with theory. The observed neutron count reported by Naranjo *et al.* [10] was 15 300 neutrons per cycle, which amounts to 85 000 total source neutrons after accounting for their reported detection efficiency of $\eta = 0.18$. Our crystals had less available charge for ionization by a factor of 2.25 due to our smaller crystal radii. However, some of the discrepancy between our results and those reported by Naranjo *et al.* must be due to some advantage in ionization efficiency in the previous work. Future experiments to increase the fill gas ionization efficiency, and to accelerate the ions to higher energy, will allow the production of thermoelectric cooler-powered miniature neutron generators. The use of a tritiated target in place of a deuterated target will immediately result in a neutron yield increase of over 2 orders of magnitude due to a higher neutron production cross section. Pyroelectric acceleration can also be used for other ion-induced nuclear reactions which would otherwise require a much more expensive ion accelerator.

This work was supported by NEER Grant No. 04ID14596.

*Electronic address: geuthj@rpi.edu

[1] Sidney B. Lang, *Sourcebook of Pyroelectricity* (Gordon and Breach, New York, 1974).
[2] G. Rosenman, D. Shur, Ya. E. Krasik, and A. Dunaevsky, J. Appl. Phys. **88**, 6109 (2000).
[3] Jeffrey Geuther, Yaron Danon, Frank Saglime, and Bryndol Sones, in *Abstracts from the Sixth International Meeting on Nuclear Applications of Accelerator Technology, San Diego, CA* (American Nuclear Society, LaGrange, IL, 2003), p. 124.
[4] J. A. Geuther and Y. Danon, J. Appl. Phys. **97**, 104916 (2005).
[5] Interpreted ENDF file, http://t2.lanl.gov/cgi-bin/endf?3,50,/inet/WWW/data/data/ENDF-deuteron/H/dd.
[6] J. D. Brownridge, Nature (London) **358**, 287 (1992).
[7] http://www.amptek.com.
[8] J. D. Brownridge and S. M. Shafroth, Appl. Phys. Lett. **79**, 3364 (2001).
[9] J. A. Geuther and Y. Danon, J. Appl. Phys. **97**, 074109 (2005).
[10] B. Naranjo, J. K. Gimzewski, and S. Putterman, Nature (London) **434**, 1115 (2005).
[11] Y. Danon, project abstract, "A Novel Compact Pyroelectric X-Ray and Neutron Source," DOE NEER Grant No. 04ID14596, 2004, http://neer.inel.gov/abstract.asp?ProjectID=126.
[12] Jeffrey Geuther and Yaron Danon *Transactions of the ANS Annual Meeting, San Diego, CA* (American Nuclear Society, LaGrange, IL, 2005), p. 775.
[13] Jeffrey Geuther and Yaron Danon, *Transactions of the ANS Winter Meeting, Washington, DC* (American Nuclear Society, LaGrange, IL, 2004), p. 885.
[14] J. D. Brownridge and S. Raboy, J. Appl. Phys. **86**, 640 (1999).
[15] http://www.fullam.com.
[16] J. H. Lee and C. S. Lee, Nucl. Instrum. Methods Phys. Res., Sect. A **402**, 147 (1998).
[17] J. K. Dickens, computer code SCINFUL, ORNL-6462, 1988; NEA Data Bank Program No. PSR-0267, 1994 (unpublished).
[18] Glenn F. Knoll, *Radiation Detection and Measurement* (Wiley, New York, 2000), 3rd. ed
[19] J. F. Ziegler and J. P. Biersack, computer code SRIM2003, The Stopping and Range of Ions in Matter, Version 2003.20, 2003.